Dalton Transactions

Accepted Manuscript

ROYAL SOCIETY OF CHEMISTRY

www.rsc.org/dalton

Dalton Transactions

Cite this: DOI: 10.1039/c0xx00000x

www.rsc.org/dalton

PERSPECTIVE

Electron transfer and catalysis with high-valent metal-oxo complexes

Shunichi Fukuzumi

Received (in XXX, XXX) Xth XXXXXXXXX 20XX, Accepted Xth XXXXXXXXX 20XX
DOI: 10.1039/b000000x

High-valent metal-oxo complexes are produced by reductive activation of dioxygen via reduction of metal complexes with reductants and dioxygen. Photoinduced electron transfer from substrates to metal complexes with dioxygen also leads to generation of high-valent metal-oxo complexes that can oxygenate substrates. In such a case metal complexes act as a photocatalyst to oxygenate substrates with dioxygen. High-valent metal-oxo complexes are also produced by proton-coupled electron-transfer oxidation of metal complexes by one-electron oxidants with water, oxygenating substrates to regenerate metal complexes. In such a case metal complexes act as a catalyst for electron-transfer oxygenation of substrates by one-electron oxidants with water that acts as an oxygen source. The one-electron oxidants which can oxidize metal complexes can be replaced by much weaker oxidants by combination of redox photocatalysts and metal complexes. Thus, photocatalytic oxygenation of substrates proceeds via photoinduced electron transfer from a photocatalyt to reductants followed by proton-coupled electron transfer oxidation of metal complexes with the oxidized photocatalyst to produce high-valent metal-oxo complexes that oxygenate substrates. Thermal and photoinduced electron-transfer catalytic reactions of high-valent metal-oxo complexes for oxygenation of substrates using water or dioxygen as an oxygen source are summarized in this perspective.

Shunichi Fukuzumi

Shunichi Fukuzumi earned a PhD. degree in applied chemistry at Tokyo Institute of Technology in 1978. After working as a postdoctoral fellow (1978-1981) at Indiana University in USA, he joined the Department of Applied Chemistry, Osaka University, as an Assistant Professor in 1981 and was promoted to a Full Professor in 1994. He is now a Distinguished Professor at Osaka University and the director of an ALCA (Advanced Carbon Technology Research and Development) project.

1. Introduction

Heme-containing enzymes such as cytochrome P450 peroxidases and catalases catalyse many important metabolic oxidation reactions by dioxygen.[1-3] The remarkable catalytic reactivity is derived from an iron(IV)-oxo porphyrin π-radical cation (compound I), which is the ultimate oxidant in these enzymatic oxidation reactions. Generation of compound I in P450 requires two electrons and protons to activate dioxygen (O_2) as shown in eqn (1).[3-8] An iron(IV)-oxo porphyrin π-radical cation [compound I: $(P^{\bullet+})Fe^{IV}(O)$] derived from horseradish peroxidase (HRP) is produced by the reaction with H_2O_2, which is the two-electron reduction product of O_2.[9-11]

$$(P)Fe^{III} + O_2 + 2e^- + 2H^+ \rightarrow (P^{\bullet+})Fe^{IV}(O) + H_2O \quad (1)$$

Groves et al. were the first to report cytochrome P450-type activity in a model system using iron(III) tetraphenylporphyrin chloride [$(TPP)Fe^{III}(Cl)$] and iodosylbenzene (PhIO) as an oxidant which can oxidize the Fe(III) porphyrin directly to produce $[(TPP)Fe^{IV}(O)]^{\bullet+}$ in a so called "shunt" pathway.[12] Since then synthetic models of compound I have provided valuable mechanistic insight into the molecular catalytic mechanism of P450.[13-18] Non-heme iron-dependent oxygenases are also known to catalyse oxidative transformations with a high degree of selectivity and catalytic efficiency.[18-24]

Among high-valent metal-oxo species, $Mn^V(O)$ species have merited special attention, because they are postulated as important intermediates in conversion of water to dioxygen during water oxidation in photosynthesis.[25-30] In this case, the generation of $Mn^V(O)$ requires abstraction of two electrons and two protons from water [eqn (2)], which is opposite to the case in

$$Mn^{III} + H_2O - 2e^- - 2H^+ \rightarrow Mn^V(O) \quad (2)$$

eqn (1). Groves and co-workers reported the first preparation of a $Mn^V(O)$ complex in the reaction of a water-soluble

[a]*Department of Material and Life Science, Division of Advanced Science and Biotechnology, Graduate School of Engineering, Osaka University, ALCA, Japan Science and Technology Agency (JST), Suita, Osaka 565-0871, Japan. Fax: +81-6-6879-7370; Tel: +81-6-6879-7368; E-mail: fukuzumi@chem.eng.osaka-u.ac.jp*

manganese(III) porphyrin with active oxygen donors such as *m*-chloroperoxybenzoic acid (*m*CPBA), oxone, and OCl^- in aqueous solution.[31] Since then there are several additional examples of $Mn^V(O)$ sepcies with macrocyclic ligands.[32-35] However, active oxygen donors such as PhIO, H_2O_2 and *m*CPBA have been normally used for the catalytic oxygenation of substrates using high-valent metal-oxo species.

This perspective article reviews generation of high-valent metal-oxo species derived from O_2 with two electrons protons (eqn (1)) as well as from H_2O by abstracting two electrons and protons (eqn (2)) and the catalytic oxygenation of substrates with high-valent metal-oxo species.

2. Reductive dioxygen activation by metal complexes

2.1. Direct dioxygen activation

A chromium(V)-oxo complex ([(tpfc)Cr^V(O)]: tpfc = tris(pentafluorophenyl)corrole) in Scheme 1) was formed by the direct reaction of [(tpfc)Cr^{III}] and O_2.[36,37] Although electron transfer from [(tpfc)Cr^{III}] (E_{ox} = 0.37 V vs SCE)[36] to O_2 (E_{red} = –0.86 V vs SCE)[38] is highly engergonic, the strong binding of $O_2^{\bullet-}$ to [(tpfc)Cr^{IV}]$^+$ makes formation of the suproxo complex ([(tpfc)$Cr^{IV}(O_2)$]) energetically possible (eqn (3)). Electron transfer from [(tpfc)Cr^{III}] to [(tpfc)$Cr^{IV}(O_2)$] occurs to produce the dinuclear peroxo complex ([(tpfc)$Cr^{IV}(O_2)Cr^{IV}$(tpfc)]) (eqn (4)).[36] The homolytic cleavage of the O–O bond yields the oxo complex ([(tpfc)Cr^V(O)]) (eqn (5)).[36] Thus, [(tpfc)Cr^V(O)] is

Scheme 1

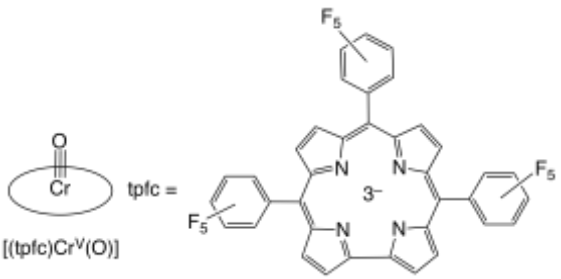

$$[(tpfc)Cr^{III}] + O_2 \rightleftharpoons [(tpfc)Cr^{IV}(O_2)] \quad (3)$$

$$[(tpfc)Cr^{III}] + [(tpfc)Cr^{IV}(O_2)] \rightarrow [(tpfc)Cr^{IV}(O_2)Cr^{IV}(tpfc)] \quad (4)$$

$$[(tpfc)Cr^{IV}(O_2)Cr^{IV}(tpfc)] \rightarrow [(tpfc)Cr^{V}(O)] \quad (5)$$

formed by direct oxidation of [(tpfc)Cr^{III}] with O_2 without addition of electrons or protons in contrast to the case in eqn (1). The rate-determining step for formation of [(tpfc)Cr^V(O)] is the initial electron transfer from [(tpfc)Cr^{III}] to O_2, when no intermediates such as [(tpfc)$Cr^{IV}(O_2)$] or [(tpfc)$Cr^{IV}(O_2)Cr^{IV}$(tpfc)] can be observed.[36]

Because [(tpfc)Cr^V(O)] can oxidize triphenylphosphine (Ph_3P) to produce triphenylphosphine oxide (Ph_3PO) and regenerate [(tpfc)Cr^{III}], [(tpfc)Cr^{III}] acts as a catalyst for oxygenation of Ph_3P with O_2 (eqn (6)).[37]

$$Ph_3P + (1/2)O_2 \xrightarrow[[(tpfc)Cr^{III}]]{} Ph_3PO \quad (6)$$

Direct O_2 activation also occurred with a trianionic pincer chromium(III) complex ([^{t}BuOCO]$Cr^{III}(THF)_3$: ^{t}BuOCO = [2,6-(^{t}Bu$C_6H_3O)_2C_6H_3]^{3-}$, THF = tetrahydrofuran) as shown in Scheme 2.[39] In this case, the dissociation of the THF ligand is required for the reaction of the Cr^{III} complex with O_2.[39]

Scheme 2

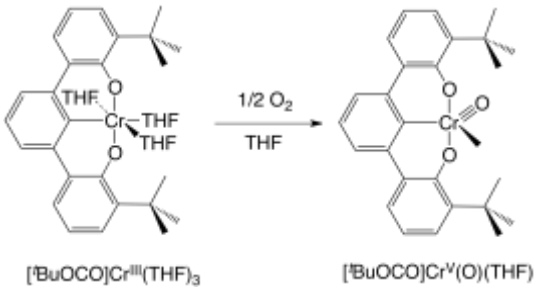

2.2. Dioxygen activation with an NADH analogue

Formation of a non-heme iron(IV)-oxo complex by the reductive activation of O_2 with an NADH (dihydronicotinamide adenine dinucletoide) analogue was reported for the reaction of [(TMC)Fe^{II}]$^{2+}$ (TMC = tetramethyl-1,4,8,11-tetraazacyclotetradecane) with 1-benzyl-1,4-dihycronicotinamide (BNAH) and $HClO_4$ in acetonitirile (MeCN) at 298 K (eqn (7)).[40] The O_2

Scheme 2

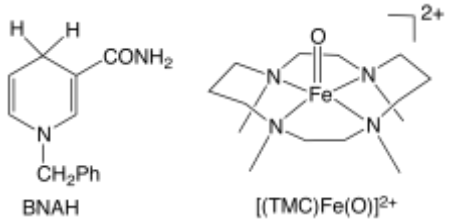

$$BNAH + [(TMC)Fe^{II}]^{2+} + O_2 + H^+ \rightarrow BNA^+ + [(TMC)Fe^{IV}(O)]^{2+} + H_2O \quad (7)$$

activation occurs via proton-coupled electron transfer (PCET) from [(TMC)Fe^{II}]$^{2+}$ to O_2 with H^+ to produce [(TMC)Fe^{IV}(OOH)]$^{3+}$ [eqn (8)].[40] Electron transfer from [(TMC)Fe^{II}]$^{2+}$ to O_2 is highly endergonic judging from the one-electron oxidation potential of [(TMC)Fe^{II}]$^{2+}$ (E_{ox} = 0.38 V vs SCE) and the one-electron reduction potential of O_2 (E_{red} = –0.86 V vs SCE) in MeCN.[38] In the presence of $HClO_4$ (0.10 M), however, the one-electron reduction potential was positively shifted to –0.21 V vs SCE because of the protonation of $O_2^{\bullet-}$, when proton-coupld electron transfer (PCET) from 1,1'-diemthylferrocene (E_{ox} = 0.28 V) to O_2 occurs, resulting the two-electron redction of O_2 in the presence of $HClO_4$ to produce the ferrocenium ion and H_2O_2.[41] Thus, PCET from [(TMC)Fe^{II}]$^{2+}$ to O_2 also occurs, followed by the binding of $HO_2^{\bullet}$ to [(TMC)Fe^{II}]$^{3+}$ to produce a putative high-valent species ([(TMC)Fe^{IV}(OOH)]$^{3+}$), the formaton of which may be still endergonic. However, the subsequent facile two-electron reduction of [(TMC)Fe^{IV}(OOH)]$^{3+}$

by BNAH may be thermodynamically feasible to produce $[(TMC)Fe^{II}]^{2+}$ and hydrogen peroxide (H_2O_2) [eqn (9)].[28] The reaction of $[(TMC)Fe^{II}]^{2+}$ with H_2O_2 yields $[(TMC)Fe^{IV}(O)]$ and water [eqn (10)].[40]

$$[(TMC)Fe^{II}]^{2+} + O_2 + H^+ \rightleftharpoons [(TMC)Fe^{IV}(OOH)]^{3+} \quad (8)$$

$$BNAH + [(TMC)Fe^{IV}(OOH)]^{3+} \rightarrow BNA^+ + [(TMC)Fe^{II}]^{2+} + H_2O_2 \quad (9)$$

$$[(TMC)Fe^{II}]^{2+} + H_2O_2 \rightarrow [(TMC)Fe^{IV}(O)]^{2+} + H_2O \quad (10)$$

In the presence of excess BNAH, hydride transfer from BNAH to $[(TMC)Fe^{IV}(O)]^{2+}$ occurs to produce BNA^+ and regenerate $[(TMC)Fe^{II}]^{2+}$ [eqn (11)].[42] Thus, $[(TMC)Fe^{II}]^{2+}$ can catalyse the

$$BNAH + [(TMC)Fe^{IV}(O)]^{2+} + H^+ \rightarrow BNA^+ + [(TMC)Fe^{II}(OH)]^+ + H_2O \quad (11)$$

four-electron reduction of O_2 by BNAH in the presence of H^+ [eqn (12)].

$$2BNAH + O_2 + 2H^+ \rightarrow 2BNA^+ + H_2O \quad (12)$$
$$[(TMC)Fe^{IV}(O)]^{2+}$$

2.3. Dioxygen activation with electrons and protons

Hydrogen donors such as alcohols and alkenes (RH) can also ben utilized in the reductive activation of O_2 to produce $[(TMC)Fe^{IV}(O)]^{2+}$ [eqn (13)].[43] In this case, no proton is required

$$RH + [(TMC)Fe^{II}]^{2+} + O_2 \rightarrow ROH + [(TMC)Fe^{IV}(O)]^{2+} \quad (13)$$

For the O_2 activation. Electron transfer from $[(TMC)Fe^{II}]^{2+}$ to O_2 to produce the superoxo complex $[(TMC)Fe^{III}(O_2)]^{2+}$ [eqn (14)] is followed by hydrogen atom transfer from RH to produce $R^\bullet$ and the hydroperoxo complex $[(TMC)Fe^{III}(OOH)]^{2+}$ in the cage [eqn (15)].[43] The facile radical reaction of $R^\bullet$ with $[(TMC)Fe^{III}(OOH)]^{2+}$ in the cage yields ROH and $[(TMC)Fe^{IV}(O)]^{2+}$ [eqn (16)].[43] Although the formation of

$$[(TMC)Fe^{II}]^{2+} + O_2 \rightleftharpoons [(TMC)Fe^{III}(O_2)]^{2+} \quad (14)$$

$$RH + [(TMC)Fe^{III}(O_2)]^{2+} \rightarrow (R^\bullet\ [(TMC)Fe^{III}(OOH)]^{2+}) \quad (15)$$

$$(R^\bullet\ [(TMC)Fe^{III}(OOH)]^{2+}) \rightarrow ROH + [(TMC)Fe^{IV}(O)]^{2+} \quad (16)$$

$[(TMC)Fe^{III}(O_2)]^{2+}$ [eqn (14)] is uphill, the subsequent hydrogen atom trasnfer [eqn (15)] and the radical reaction [eqn (16)] make the O_2 activation possible.[43] The rate determining stp is the hydrogen atom transfer [eqn (15)] as indicated by the large deuterium kinetic isotope effect (KIE = 6.3(3) for RH = cyclohexene).[43]

Carbon-centered radical ($R^\bullet$) produced in the reaction of $[(TMC)Fe^{III}(O_2)]^{2+}$ with RH also reacts with O_2 to produce $ROO^\bullet$ [eqn (17)] which abstracts hydrogen from RH to produce ROOH and regenerate $R^\bullet$ [eqn (18)]. $[(TMC)Fe^{II}]^{2+}$ reacts with ROOH to produce $[(TMC)Fe^{IV}(O)]^{2+}$ and ROH [eqn (19)]. Such an autoxidation pathway becomes dominant for RH = isopropanol and *cis*-1,2-dimethylcyclohexane when the C-H bond dissociation energy of RH (isorpropanol = 94.0 kcal mol^{-1} and *cis*-1,2-dimethylcyclohexane = 96.5 kcal mol^{-1})[44] is significantly higher than cyclohexene (88.8 kcal mol^{-1}).[45,46]

$$R^\bullet + O_2 \rightarrow ROO^\bullet \quad (17)$$

$$ROO^\bullet + RH \rightarrow ROOH + R^\bullet \quad (18)$$

$$[(TMC)Fe^{II}]^{2+} + ROOH \rightarrow [(TMC)Fe^{IV}(O)]^{2+} + ROH \quad (19)$$

Formation of $[(TMC)Fe^{IV}(O)]^{2+}$ in the reaction of $[(TMC)Fe^{II}]^{2+}$ with tetraphenylborate (BPh_4^-) used as an electron soruce and water with Sc^{3+} as a proton souce also proceeds via an autoxidation pathway as shown in Scheme 3,[47] rather than direct O_2 activation with BPh_4^- and Sc^{3+}.[48] The radical chain reaction is initiatd by Sc^{3+}–promoted electron transfer from BPh_4^- to $[(TMC)Fe^{IV}(O)]^{2+}$ to produce $Ph^\bullet$, BPh_3, and the $[(TMC)Fe^{III}(O)]^+$–Sc^{3+} complex.[47,49] Phenyl radical ($Ph^\bullet$) reacts rapidly with O_2 to produce the peroxyl radical ($PhOO^\bullet$).[50,51] Then, Sc^{3+}–promoted electron transfer from BPh_4^- to $PhOO^\bullet$ occurs as a chain propagation step to produce BPh_3 and the $PhOO^-/Sc^{3+}$ complex, accompanied by regeneration of $Ph^\bullet$. The $PhOO^-/Sc^{3+}$ complex reacts with $[(TMC)Fe^{II}]^{2+}$ to produce $[(TMC)Fe^{IV}(O)]^{2+}$ and PhOH after the reaction with residual water (Scheme 3).[47]

Scheme 3

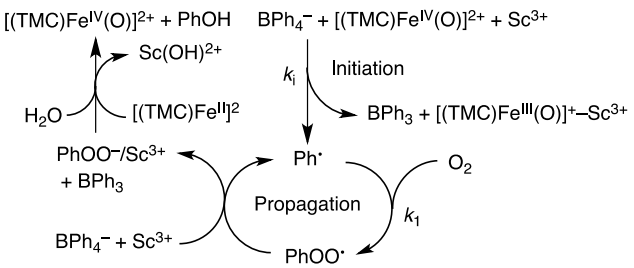

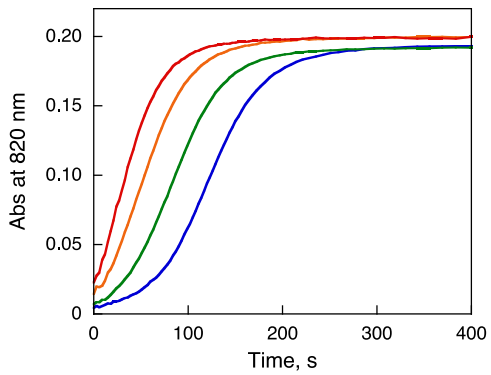

Fig. 1 Time courses of the absorption change monitored at 820 nm for formation of $[(TMC)Fe^{IV}(O)]^{2+}$ in the reactions of $[(TMC)Fe^{II}]2+$ (0.50 mM) with $NaBPh_4$ (1.0 mM) and $Sc(OTf)_3$ (1.0 mM) in the absence and presence of a catalytic amount of $[(TMC)Fe^{IV}(O)]^{2+}$ (blue: 0 M, green: 10 μM, orange: 25 μM, red: 50 μM) in O_2-saturated MeCN at 298 K.

The autocatalytic behavior was confirmed by the effect of a catalytic amount of $[(TMC)Fe^{IV}(O)]^{2+}$, which initiate the radical chain reaction in Scheme 3 as shown in Fig. 1, where the induction period decreases with inreasing a catalytic amount of

$[(TMC)Fe^{IV}(O)]^{2+}$. Such an autocatalytic behavior was also confirmed by the effect of a catalytic amount of Cp_2Fe, which can reduce $[(TMC)Fe^{IV}(O)]^{2+}$,[52,53] and the induction period increased with an increase in concentration of Cp_2Fe.[47]

2.4. Photoinduced O_2 activation

As mentioned above, dioxygen activation is started by electron transfer from metal complexes to O_2. Photoexcitation of metal complexes enhances the electron donor ability of metal complexes by the excitation energy. Thus, visible light photoirradiation of an oxygen-saturated benzonitrile solution of a manganese(III) corrolazine complex $[(TBP_8Cz)Mn^{III}$: [TBP_8Cz = octakis(*p*-tert-butylphenyl)corrolazinato^{3-}] in the presence of toluene derivatives in benzonitirle resulted in formation of the manganese(V)-oxo complex $[(TBP_8Cz)Mn^{V}(O)]$.[54,55] In the dark, no reaction of $(TBP_8Cz)Mn^{III}$ occurred with O_2 and toluene derivatives.[54] The mechanism of photoinduced O_2 activation with $(TBP_8Cz)Mn^{III}$ and toluene is shown in Scheme 4.[55] Photoexcitation of $(TBP_8Cz)Mn^{III}$ resulted in formation of the tripquintet excited state ($^5T_1$), which underwent intersystem crossing (ISC) to produce the tripseptet excited state ($^7T_1$) as revealed by femtosecond laser flash photolysis measurements.[55-57] Because the one-electron oxidation potential of $[(TBP_8Cz)Mn^{III}]^*$ ($^7T_1$) (–0.90 V vs SCE) is more negative than the one-electon reduction potential of O_2 (–0.87 V vs SCE), electron transfer from $[(TBP8Cz)Mn^{III}]^*$ ($^7T_1$) to O_2 occurs efficiently to produce the Mn(IV)-superoxo complex ($[(TBP_8Cz)Mn^{IV}(O_2^{\bullet-})]$) with the diffusion-limited rate constant.[55]

Scheme 4

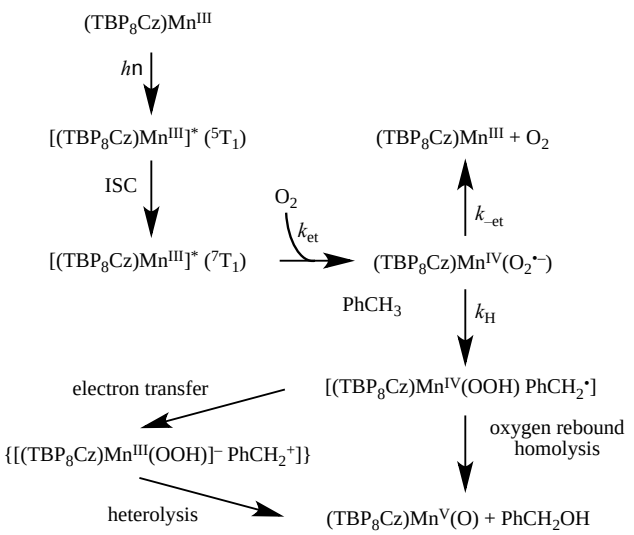

The binding of $O_2^{\bullet-}$ to $[(TBP_8Cz)Mn^{IV}]^+$ facilitates the electron-transfer reaction, because the electron-transfer product is more stabilized thermodynamically. In the presence of toluene, hydrogen atrom transfer from toluene to $[(TBP_8Cz)Mn^{IV}(O_2)]$ occurs to produce benzyl radical and the hydroperoxo complex $[(TBP_8Cz)Mn^{IV}(OOH)]$.[55] As the case of the reaction of $R^{\bullet}$ with $[(TMC)Fe^{III}(OOH)]^{2+}$ in the cage [eqn (16)],[40] the reaction of benzyl radical with $[(TBP_8Cz)Mn^{IV}(OOH)]$ yields benzyl alcohol and $[(TBP_8Cz)Mn^{V}(O)]$.[55] The rate-determining step in the catalytic cycle in Scheme 4 is hydrogen atrom transfer from toluene to $[(TBP_8Cz)Mn^{IV}(O_2)]$ in competition with the intramolecular back electron transfer from $O_2^{\bullet-}$ to the Mn^{IV} moiety to produce $(TBP_8Cz)Mn^{III}$ and O_2, as evidenced by the large dueterium kinetic isotope effects (KIE = 5.4 and 5.3 for toluene and mesitylene, respectively).[55]

When toluene derivatives were replaced by 10-methyl-9,10-dihydroacrridine ($AcrH_2$), manganese(III) porphyrins $[(P)Mn^{III}]$ as well as $(TBP_8Cz)Mn^{III}$ act as photocatalysts for oxygenation of $AcrH_2$ by O_2 in benzonitrile to yield 10-methylacridone (Acr=O) as shown in Scheme 5.[58] After photoexcitation of $(P)Mn^{III}$, the

Scheme 5

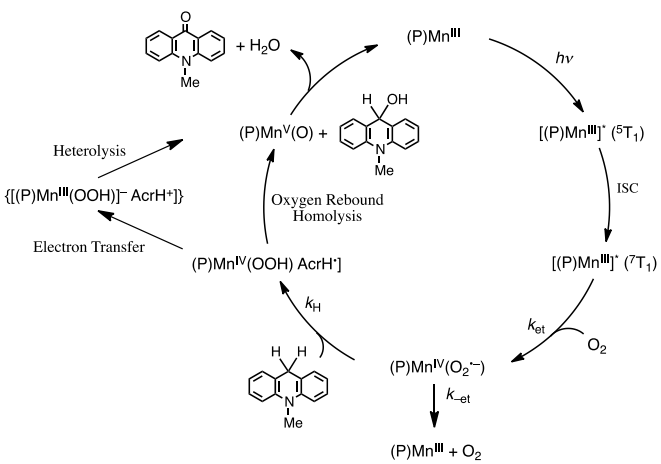

tripquintet excited state ($^5T_1$)) is produced and converted rapidly to the tripseptet excited state ($^7T_1$) by intersystem crossing, followed by electron transfer from $^7T_1$ to O_2 to produce the superoxo complex $[(P)MnIV(O_2^{\bullet-})]$.[58] As the case of $(TBP_8Cz)Mn^{III}$ in Scheme 4, hydrogen-atom transfer (HAT) from $AcrH_2$ to $(P)Mn^{IV}(O_2^{\bullet-})$ occurs to produce the hydroperoxo complex $[(P)Mn^{IV}(OOH)]$ and acridinyl radical ($AcrH^{\bullet}$), which is the rate-determining step of overall reaction, as reveaed by a large KIE value of 22.[58] The subsequent O–O bond cleavage by $AcrH^{\bullet}$ occurs rapidly inside the reaction cage before the reaction of $AcrH^{\bullet}$ with O_2 to yield $(P)Mn^{V}(O)$ and 9-hydroxy-10-methyl-9,10-dihydroacridine [AcrH(OH)].[58] Hydride and proton transfer from AcrH(OH) to $(O)Mn^{V}(O)$ occurs to yield Acr=O, accompanied by regeneration of $(P)Mn^{III}$.[58]

3. Oxidative water activation by metal complexes

3.1. Electron-transfer oxidation of metalloporphyrins

The two-electron oxidation of a manganese(III) porphyrin ($(TMP)Mn^{III}(OH)$: TMP^{2-} = 5,10,15,20-tetrakis(2,4,6-trismethylphenyl)porphyrin dianion) by $[Ru(bpy)_3]^{3+}$ (bpy = 2,2'-bipyridine) occurs in a stewpwise manner as shown in eqns (20) and (21).[59] The first electron transfer from $[(TMP)Mn^{III}(OH)]^+$ to

$$(TMP)Mn^{III}(OH) + [Ru(bpy)_3]^{3+} \rightarrow (TMP)Mn^{IV}(O) + [Ru(bpy)_3]^{2+} + H^+ \quad (20)$$

$$(TMP)Mn^{IV}(O) + [Ru(bpy)_3]^{3+} \rightarrow [(TMP)Mn^{V}(O)]^+ + [Ru(bpy)_3]^{2+} \quad (21)$$

$[Ru(bpy)_3]^{3+}$ is accompanied by the deprotonation to produce $(TMP)Mn^{IV}(O)$ [eqn (20)].[59] $(TMP)Mn^{IV}(O)$ is further oxidized by $[Ru(bpy)_3]^{3+}$ to produce $[(TMP)Mn^{V}(O)]^{+}$ [eqn (21)].[59]

Because $[(P)Mn^{V}(O)]^{+}$ can oxygenate a substrate (S) to yield SO in the presence of H_2O to regenerate $(P)Mn^{III}(OH)$, manganese porphyrins act as catalysts for oxygenation of substrates by $[Ru(bpy)_3]^{3+}$ with water that is the oxygen source as shown in Scheme 6.[59] The epoxidation of styrene and the

Scheme 6

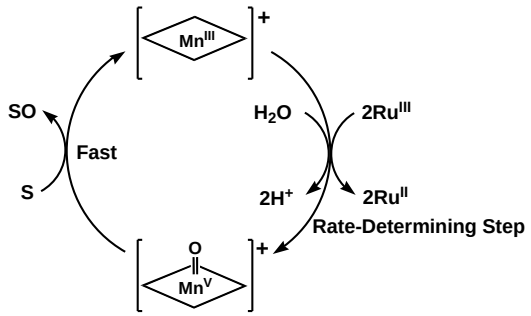

hydroxylation of ethylbenzene with $[Ru(bpy)_3]^{3+}$ in the presence of 95 % ^{18}O-water containing a catalytic amount of manganese porphyrin afforded the corresponding epoxide and alcohol with 90 % incorporation of ^{18}O in the oxygenated products.[59] Thus, the oxygen source in the oxygenated products in the manganese porphyrin-catalysed electron-transfer oxygenation of substrates with $[Ru(bpy)_3]^{3+}$ has been confirmed to be water in the mixed solvent ($MeCN/H_2O$).

Turover numbers (TONs) of the catalytic oxygenation of substrates depend on the type of manganese porphyrins due to the difference in their oxidation potentials and the steric bulkiness of the porphyrin ligand (Table 1).[59] TONs of epoxidation of cyclohexene are larger than those of styrene, probably because of

Table 1. Turnover numbers in oxygenation of cyclohexene (5.0×10^{-3} M) with $[Ru(bpy)_3]^{3+}$ (1.0×10^{-2} M), catalysed by various manganese porphyrins in CD_3CN/D_2O (9:1 v/v) solution at 298 K.

catalyst	Ar	TON cyclohexene	TON styrene
$(TMP)Mn^{III}(Cl)$		130	20
$[(TMP)Mn^{III}(H_2O)_2](PF_6)$		170	65
$(TDCPP)Mn^{III}(Cl)$		160	70
$[(TDCPP)Mn^{III}(H_2O)_2](PF_6)$		210	85
$(TMOPP)Mn^{III}(Cl)$	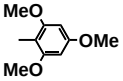	80	trace
$[(TMOPP)Mn^{III}(H_2O)_2](PF_6)$		110	35
$(DTMP)Mn^{III}_2(Cl)_2$		20	trace
$[(DTMP)Mn^{III}_2(H_2O)_2](PF_6)_2$		80	20

the stronger steric repulsion of styrene against the bulky TMP ligand of $[(TMP)Mn^{V}(O)]^{+}$ as compared with that of cyclohexene. In the case of TDCPP ligand, the oxygenation of cyclohexene and styrene is more reactive than TMP ligand because of the less steric effect of the TDCPP ligand as compared with the TMP ligand and high redox potentials.[59]

3.2. Electron-transfer oxidation of a non-heme iron(III) complex

The one-electron oxidation potential of an iron(III)-oxo complex ($[Fe^{III}H_3buea(O)]^{-}$) is quite negative to be –0.90 V *vs.* $[Cp_2Fe]^{+}/Cp_2Fc$.[60] In such case, electron transfer from an iron(III)-oxo complex ($[Fe^{III}H_3buea(O)]^{-}$) to ferrocenium cation ($[Cp_2Fc]^{+}$) rapidly occurs in DMF at –60 °C to produce the corresponding iron(IV)-oxo complex ($[Fe^{IV}H_3buea(O)]^{-}$) (Scheme 7).[61] Electron transfer from an iron(III)-hydroxo complex ($[Fe^{III}H_3buea(OH)]^{-}$) to $[Cp_2Fc]^{+}$ also occurs in DMF at -60 °C to produce the corresponding iron(IV)-oxo complex ($[Fe^{IV}H_3buea(O)]^{-}$) with concomitant deprotonation (Scheme 7).[61] Thus, the same oxoiron(IV) species was obtained from the independent oxidation of either a monomeric Fe^{III}–OH or Fe^{III}–O complex. The X-ray crystal structure of $[Fe^{IV}H_3buea(O)]^{-}$ has the trigonal bipyramidal coordination geometry with the terminal oxo ligand (O1) positioned trans to the apical N1 atom as shown in Fig. 2.[60] The Fe1–O1 bond length is 1.680(1) Å, which is slightly longer than values found for other synthetic nonheme

Scheme 7

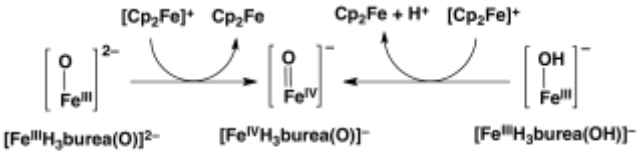

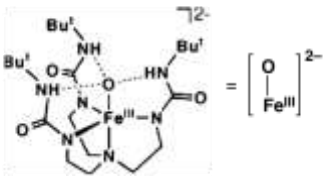

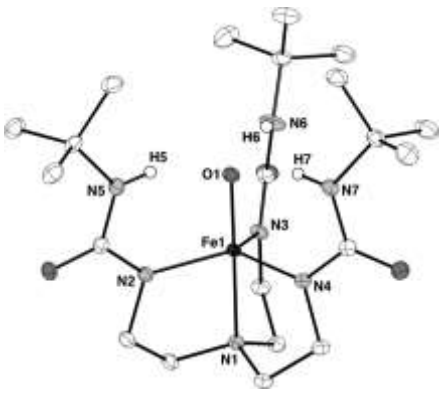

Fig. 2 Thermal ellipsoid diagram of $[Fe^{IV}H_3buea(O)]^{-}$. The ellipsoids are drawn at the 50% probability level, and non-urea hydrogen atoms are omitted for clarity.

oxoiron(IV) complexes due to the H-bonding network that surrounds the Fe^{IV}–O unit, which is absent in other systems.[62-64] The spin state of $[Fe^{IV}H_3buea(O)]^{-}$ was determined to be S = 2

based on parallel-mode X-band EPR, which showed a sharp resonance at g = 8.19 that is indicative of an S= 2 spin manifold.[61]

A non-heme iron(IV)-oxo complex, $[(N4Py)Fe^{IV}(O)]^{2+}$ (N4Py = *N*,*N*-bis(2-pyridylmethyl)-*N*-bis(2-pyridyl)methylamine) is also produced by stepwise electron-transfer oxidation of the corresponding iron(III)-hydroxo complex, $[(N4Py)Fe^{II}]^{2+}$ with $[Ru(bpy)_3]^{3+}$ (Scheme 8).[65] The second-order rate constant of

Scheme 8

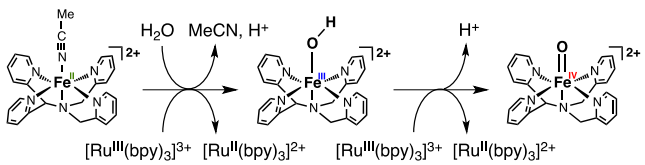

electron transfer from $[(N4Py)Fe^{III}(OH)]^{2+}$ to $[Ru(bpy)_3]^{3+}$ coupled with deprotonation increased linearly with increasing concentrations of proton acceptors (PA) in MeCN [eqn (22)].[65]

$$d[Fe^{IV}(O)]/dt = k_{PA}[Fe^{III}(OH)][Ru(bpy)_3{}^{3+}][PA] \quad (22)$$

The rate constant with PA (k_{PA}) increases with increasing the basicity of PA (K_b) as shown in Fig. 3a.[65] When H_2O was replaced by D_2O in electron transfer from $[(N4Py)Fe^{III}(OH)]^{2+}$ to $[Ru(bpy)_3]^{3+}$ in the presence of PA, deuterium kinetic isotope effects were obseved and the KIE value increases with increasing the K_b vlaue of PA (Fig. 3b).[65] The observation of KIE suggests that the O–H bond cleavage of $[(N4Py)Fe^{III}(OH)]^{2+}$ is involved in the rate-determining step of formation of $[(NePy)Fe^{IV}(O)]^{2+}$ via electron-transfer oxidation of $[(N4Py)Fe^{III}(OH)]^{2+}$ by $[Ru(bpy)_3]^{3+}$ with PA.[65]

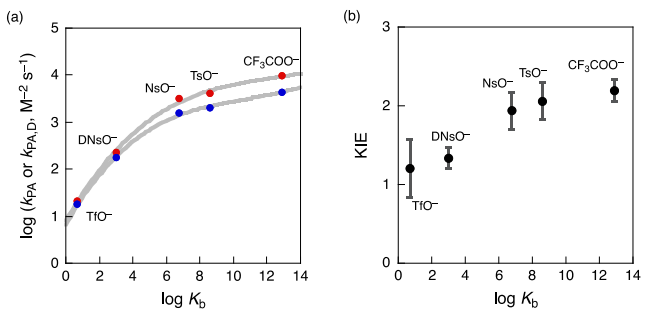

Fig. 3 (a) Plots of log k_{PA} and $k_{PA,D}$ for electron transfer from $[(N4Py)Fe^{III}(OH)]^{2+}$ to $[Ru(bpy)_3]^{3+}$ with PA in the presence of 0.56 M H_2O (red points) and D_2O (blue points) at 298 K vs log K_b of PA. (b) Plot of KIE vs log K_b.

A coordinatively saturated ruthenium(II) complex having tetradentate tris(2-pyridylmethyl)amine (TPA) and bidentate diimine ligands such as 2,2'-bipyridine (bpy), $[(TPA)(bpy)Ru]^{2+}$ was oxidized by a Ce(IV) ion to afford a Ru(IV)-oxo complex, $[(TPA\text{-}H^+)(bpy)Ru(O)]^{3+}$.[66] The crystal structure of the Ru(IV)-oxo complex was determined by X-ray crystallography as shown in Fig. 4, where the TPA ligand partially dissociates to be in a facial tridentate fashion and the uncoordinated pyridine moiety is protonated.[67] The spin state of the Ru(IV)-oxo complex, which showed paramagnetically shifted NMR signals in the range of 60 ~ –20 ppm, was determined to be an intermediate spin (S = 1).[67] The resonance Raman spectrum of $[(TPA\text{-}H^+)(bpy)Ru(O)]^{3+}$ prepared in $H_2{}^{16}O$ assigned to ν(Ru=O) at 805 cm^{-1}, which was shifted to 764 cm^{-1}, when $[(TPA\text{-}H^+)(bpy)Ru(O)]^{3+}$ was prepared in $H_2{}^{18}O$.[67] The shift value ($\Delta\nu$ = 41 cm^{-1}) agrees with the calculated value ($\Delta\nu$ = 40 cm^{-1}) for ν(Ru=O).[67]

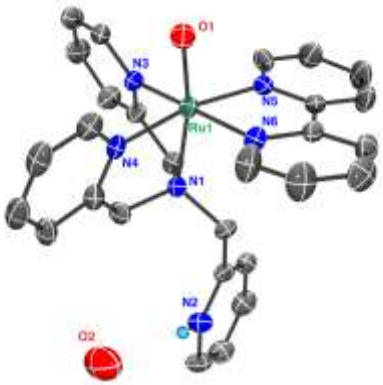

Fig. 4 An ORTEP drawing of the cation moiety of $[(TPA\text{-}H^+)(bpy)Ru(O)]^{3+}$ using 50% probability thermal ellipsoids with numbering scheme for the heteroatoms. Hydrogen atoms are omitted for clarity except the hydrogen on the uncoordinated pyridine nitrogen (N2). O2 represents the water molecule of crystallization.

Because the Ru(IV)-oxo complex can oxidize various substrates, $[(TPA)(bpy)Ru]^{2+}$ acts as an efficient catalyst for oxidaiton of alkens such as cyclohexene and alkylbenzene such as cumene, ethylbenzene and toluene.[67,68] Nonheme Mn(IV)-oxo complexes are also produced by their manganese(II) precursors using cerium(IV) ammonium nitrate as a one-electron oxidant using water as an oxygen source, acting as catalysts for oxidation of thioanisoles.[69]

3.3. Catalytic water oxidation

High-valent metal-oxo complexes are believed to act as reactive intermediates for catalytic water oxidation.[70-80] However, the catalytic mechanism for water oxidation has yet to be fully clarified. The oxidation of ligands of metal complexes during the catalytic water oxidation has precluded the detailed mechanistic study.[81-88] Mononuclear water oxidation catalysts with all inorganic ligands may be more suitable to elucidate the catalytic mechanism of water oxidation as compared with multinuclear water oxidation catalysts.[89-94] Thus, catalytic water oxidation to generate oxygen was achieved using all-inorganic mononuclear ruthenium complexes bearing Keggin-type lacunary heteropolytungstate, $[Ru^{III}(H_2O)SiW_{11}O_{39}]^{5-}$ (**1**) and $[Ru^{III}(H_2O)GeW_{11}O_{39}]^{5-}$ (**2**) (Fig. 5) as catalysts with $(NH_4)_2[Ce^{IV}(NO_3)_6]$ (CAN) that was employed as a one-electron oxidant in water.[95] The oxygen atoms of evolved oxygen were confirmed to come from water by isotope-labelled experiments.[95] Cyclic voltammetric measurements of **1** and **2** at various pH's indicate that the Ru(III) complexes are oxidized to the Ru(V)-oxo complexes with CAN.[95] The Ru(V)-oxo complex derived from **1** was detected by UV–visible absorption, EPR, and resonance

Raman measurements in situ as an active species during the water oxidation reaction.[95]

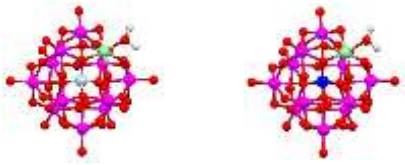

$[Ru^{III}(H_2O)SiW_{11}O_{39}]^{5-}$ (**1**) $[Ru^{III}(H_2O)GeW_{11}O_{39}]^{5-}$ (**2**)

Fig. 5 Structures of ruthenium complexes bearing Keggin-type lacunary heteropolytungstate, $[Ru^{III}(H_2O)SiW_{11}O_{39}]^{5-}$ (**1**) and $[Ru^{III}(H_2O)GeW_{11}O_{39}]^{5-}$ (**2**).

The overall catalytic mechanism of water oxidation was revealed based on the kinetic analysis and detection of the catalytic intermediates as shown in Scheme 9.[95] The catalytic water oxidation by CAN with the Ru^{III}-OH_2 complex (**1** and **2**) proceeds via the Ru^{V}=O complex, which is formed by the fast two-electron oxidation of the Ru^{III}-OH_2 complex coupled with deprotonation. The reaction of the Ru^{V}=O complex with H_2O to produce the Ru^{III}-OOH complex is the rate-determining step, followed by the fast electron-transfer oxidation of the Ru^{III}-OOH with CAN, leading to the oxygen evolution, which competes with the back reaction from the Ru^{III}-OOH complex with H^+ to regenerate the Ru^{V}=O complex.[95] The complex **2** exhibited the higher catalytic reactivity for the water oxidation with CAN than complex **1** because of the electron-withdrawing effect of germanium (core atom of the ligand).[95]

Scheme 9

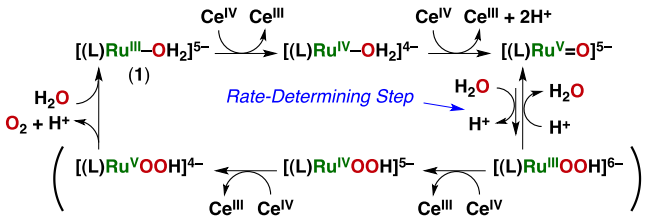

3.4 Photocatalytic oxygenation with water

Because $[Ru(bpy)_3]^{3+}$ is produced by oxidative quenching of the excited state of $[Ru(bpy)_3]^{2+}$ with a one-electron oxidant such as $[Co^{III}(NH_3)_5Cl]^{2+}$, the thermal catalytic oxygenation of substrates in Scheme 6 can be converted to the photocatalytic oxygenation of substrates with $[Ru(bpy)_3]^{2+}$ which acts as a photocatalyst as shown in Scheme 10.[96] The photocatalytic oxygenation of substrates (S) with H_2O is started by photoinduced electron transfer from the excited state of $[Ru(bpy)_3]^{2+}$ ($[Ru(bpy)_3]^{2+*}$) to $[Co^{III}(NH_3)_5Cl]^{2+}$ to produce $[Ru(bpy)_3]^{3+}$, which oxidizes $(TMPS)Mn^{III}(OH)$ to $(TMPS)Mn^{IV}(O)$. The latter intermediate disporportionates with H^+ to produce $[(TMPS)Mn^{V}(O)]^+$ and $(TMPS)Mn^{III}(OH)$. Substrates (S) are then oxygenated by $[(TMPS)Mn^{V}(O)]^+$ to yield oxygenated products (SO), accompanied by regeneration of $(TMPS)Mn^{III}(OH)$ with H_2O. In this sequence, the oxygen atom in SO was confirmed to be derived from H_2O as demonstrated by ^{18}O-labeled water experiments.[96] Because photoinduced electron transfer from $[Ru(bpy)_3]^{2+*}$ to $[Co^{III}(NH_3)_5Cl]^{2+}$ occurs in an irreversible manner without involvement of back electron transfer[97,98] and the subsequent reactions occur thermally, all photons can be used to produce the oxygenated products with the maximum quantum yield of 50%.[96]

Scheme 10

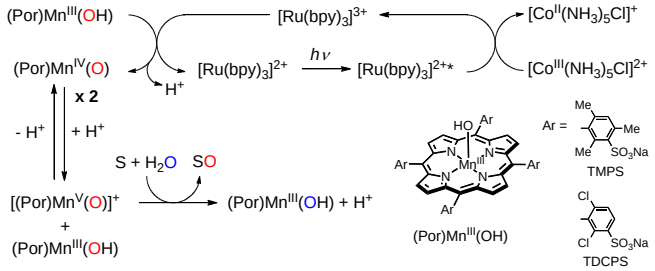

The photocatalytic formation of a non-heme iron(IV)-oxo complex ($[(N4Py)Fe^{IV}(O)]^{2+}$) also proceeds efficiently via electron transfer from $[Ru(bpy)_3]^{2+*}$ to $[Co^{III}(NH_3)_5Cl]^{2+}$ and stepwise electron-transfer oxidation of $[(N4Py)Fe^{II}]^{2+}$ with two equiv of $[Ru^{III}(bpy)_3]^{3+}$ and H_2O as an oxygen source (Scheme 11).[99] The quantum yield of formation of $[Ru^{III}(bpy)_3]^{3+}$ increased with increasing $[Co^{III}(NH_3)_5Cl]^{2+}$ concentration to reach a constant value of 80%.[98] Because $[(N4Py)Fe^{IV}(O)]^{2+}$ can oxygenate thioanisole to the sulfoxide to regenerate $[(N4Py)Fe^{II}]^{2+}$,[100,101] the combination of $[Ru(bpy)_3]^{2+}$ and $[(N4Py)Fe^{II}]^{2+}$ enabled photocatalytic oxygenation of thioanisole with $[Co^{III}(NH_3)_5Cl]^{2+}$ and H_2O.[99] Similarly photocatalytic oxidation of various substrates with $[Co^{III}(NH_3)_5Cl]^{2+}$ and H_2O occurs by combination of Ru^{II}–pyridylamine complexes and $[Ru(bpy)_3]^{2+}$.[102,103]

Scheme 11

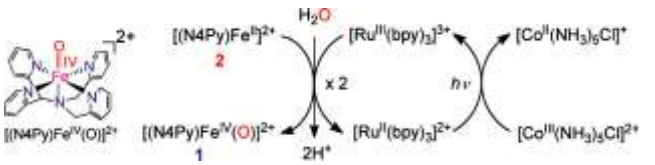

6. Conclusions

As described above, high-valent metal-oxo complexes are produced by either direct O_2 activation or reductive O_2 activation with electron and proton donors. A non-heme Fe^{II} complex react with O_2 via electron transfer from Fe^{II} to O_2, followed by binding of $O_2^{\bullet-}$ to Fe^{III} to produce the Fe^{III}–$O_2^{\bullet-}$ complex, which abstract a hydrogen from hydrogen donors (RH) to produce the Fe^{III}-OOH complex and $R^{\bullet}$. The reaction of $R^{\bullet}$ with Fe^{III}–OOH yields ROH and the $Fe^{IV}(O)$ complex in the reaction cage. When $R^{\bullet}$ is escaped from the reaction cage, the autoxidation of RH via radical chain reactions occurs to produce the hydroperoxide which reacts with the Fe^{II} complex to yield the $Fe^{IV}(O)$ complex. The electron transfer from metal complexes to O_2 is facilitated by photoexcitation of metal complexes, leading to production of high-valent metal complexes. When high-valent metal complexes can oxidize substrates, metal complexes act as photocatalysts for oxidation of substrates by O_2.

High-valent metal-oxo complexes are also produced by electron-transfer oxidation of metal-hydroxo complexes by one-electron oxidants as CAN and $[Ru(bpy)_3]^{3+}$ accompanied by deprotonation of the hydroxo moiety. When high-valent metal-oxo complexes can oxygenate substrates, metal hydroxo complexes can act as catalysts for oxygenation of substrates by one-electron oxidants with H_2O as an oxygen source. The combination of $[Ru(bpy)_3]^{2+}$ and metal hydroxo complexes constitutes a photocatalytic system for photoinduced oxygenation of substrates by one-electron oxidants with H_2O as an oxygen source. Thus, high-valent metal-oxo complexes can be produced via electron transfer oxidation of metal complexes with O_2 and H_2O, acting as catalysts for oxygenation of substrates.

Acknowledgments

The authors gratefully acknowledge the contributions of their collaborators and co-workers mentioned in the cited references, in particular Prof. Wonwoo Nam (Ewha Womans University, Korea) and Prof. Takahiko Kojima (Tsukuba University). Financial support from an ALCA project from JST is gratefully acknowledged.

References

1 T. L. Poulos, *Chem. Rev*., 2014, **114**, 3919.
2 J. Christiane, *Biochim. Biophys. Acta*, 2011, **1814**, 46.
3 F. P. Guengerich, *J. Biol. Chem*., 2013, **288**, 17063.
4 C. M. Krest, E. L. Onderko, T. H. Yosca, J. C. Calixto, R. F. Karp, J. Livada, J. Rittle, M. T. Green, *J. Biol. Chem*., 2013, **288**, 17074.
5 L. G. Denisov, T. M. Makris, S. G. Sligar and L. Schlichting, *Chem. Rev*., 2005, **105**, 2253.
6 P. R. Ortiz de Montellano, *Chem. Rev*., 2010, **110**, 932.
7 T. H. Yosca, J. Rittle, C. M. Krest, E. L. Onderko, A. Silakov, J. C. Calixto, R. K. Behan and M. T. Green, *Science*, 2013, **342**, 825.
8 J. T. Groves, *Nat. Chem*., 2014, **6**, 89.
9 U. Pérez and H. B. Dunford, *Biochim. Biophys. Acta*, 1990, **1038**, 98.
10 S. P. de Visser, S. Shaik, P. K. Sharma, D. Kumar and W. Thiel, *J. Am. Chem. Soc*., 2003, **125**, 15779.
11 O. Shoji and Y. Watanabe, *J. Biol. Inorg. Chem*., 2014, **19**, 529.
12 J. T. Groves, T. E. Nemo and R. S. Myers, *J. Am. Chem. Soc*., 1979, **101**, 1032.
13 H. L. R. Cooper and J. T. Groves, *Arc. Biochem. Bipophys*., 2010, **507**, 111.
14 B. Meunier, Chem. Rev., 1992, 92, 1411.
15 D. Ostovic and T. C. Bruice, *Acc. Chem. Res*., 1992, **25**, 314.
16 W. Nam, Y. O. Ryu and W. J. Song, *J. Biol. Inorg. Chem*., 2004, **9**, 654.
17 D. P. Goldberg, *Acc. Chem. Res*., 2007, **40**, 626.
18 W. Nam, *Acc. Chem. Res*., 2007, **40**, 522.
19 M. Costas, *Coord. Chem. Rev*., 2011, **255**, 2912.
20 C.-M. Che, V. K.-Y. Lo, C.-Y. Zhou and J.-S. Huang, *Chem. Soc. Rev*., 2011, **40**, 1950.
21 G. Yin, *Acc. Chem. Res*., 2013, **46**, 483.
22 A. Gunay, K. H. Theopold, *Chem. Rev*., 2010, **110,** 1060.
23 W. Nam, Y.-M. Lee, and S. Fukuzumi, *Acc. Chem. Res*., 2014, **47**, 1146.
24 K. Ray, F. F. Pfaff, B. Wang and W. Nam, *J. Am. Chem. Soc*., 2014, **136**, 13942.
25 M. Suga, F. Akita, K. Hirata, G. Ueno, H. Murakami, Y. Nakajima, T. Shimizu, K. Yamashita, M. Yamamoto, H. Ago and J.R. Shen, *Nature*, 2015, **517**, 99.
26 M. D. Kärkäs, O. Verho, E. V. Johnston and B. Åkermark, *Chem. Rev*., 2014, **114**, 11863.
27 G. C. Dismukes, R. Brimblecombe, G. A. N. Felton, R. S. Pryadun, J. E. Sheats, L. Spiccia and G. F. Swiegers, *Acc. Chem. Res*., 2009, **42**, 1935.
28 P. E. M. Siegbahn, *Acc. Chem. Res*., 2009, **42**, 1871.
29 R. J. Pace, R. Stranger and S. Petrie, *Dalton Trans*., 2012, **41**, 7179.
30 D. J. Vinyard, G. M. Ananyev and G. C. Dismukes, *Ann. Rev. Biochem*., 2013, **82**, 577.
31 J. T. Groves, J. Lee and S. S. Marla, *J. Am. Chem. Soc*., 1997, **119**, 6269.
32 Z. Gross, G. Golubkov and L. Simkhovich, *Angew. Chem., Int. Ed*., 2000, **39**, 4045.
33 B. S. Mandimutsira, B. Ramdhanie, R. C. Todd, H. Wang, A. A. Zareba, R. S. Czernuszewicz and D. P. Goldberg, *J. Am. Chem. Soc*., 2002, **124**, 15170.
34 S. H. Kim, H. Park, M. S. Seo, M. Kubo, T. Ogura, J. Klajn, D. T. Gryko, J. S. Valentine and W. Nam, *J. Am. Chem. Soc*., 2010, **132**, 14030.
35 K. A. Prokop, S. P. de Visser and D. P. Goldberg, *Angew. Chem., Int. Ed*., 2010, **49**, 5091.
36 A. Mahammed, H. B. Gray, A. E. Meier-Callahan and Z. Gross, *J. Am. Chem. Soc*., 2003, **125**, 1162.
37 S. Liu, K. Mase, C. Bougher, S. D. Hicks, M. M. Abu-Omar and S. Fukuzumi, *Inorg. Chem*., 2014, **53**, 7780.
38 S. Fukuzumi, S. Mochizuki and T. Tanaka, *Inorg. Chem*., 1989, **28**, 2459.
39 M. E.O'Reilly, T. J. Del Castillo, J. M. Falkowski, V. Ramachandran, M. Pati, M. C. Correia, K. A. Abboud, N. S. Dalal, D. E. Richardson and A. S. Veige, *J. Am. Chem. Soc*., 2011, **133**, 13661.
40 S. Hong, Y.-M. Lee, W. Shin, S. Fukuzumi and W. Nam, *J. Am. Chem. Soc*., 2009, **131**, 13910.
41 S. Fukuzumi, M. Chiba, M. Ishikawa, K. Ishikawa and T. Tanaka, *J. Chem. Soc., Perkin Trans. 2*, 1989, 1417.
42 S. Fukuzumi, H. Kotani, Y.-M. Lee and W. Nam, *J. Am. Chem. Soc*., 2008, **130**, 15134.
43 Y.-M. Lee, S. Hong, Y. Morimoto, W. Shin, S. Fukuzumi and W. Nam, *J. Am. Chem. Soc*., 2010, **132**, 10668.
44 S. J. Blanksby and G. B. Ellison, Acc. Chem. Res., 2003, 36, 255.
45 Y. Morimoto, Y.-M. Lee, W. Nam and S. Fukuzumi, *Chem. Commun*., 2013, **49**, 2500.
46 P. Comba, Y.-M. Lee, W. Nam, A. Waleska, *Chem. Commun*., 2014, **50**, 412.
47 Y. Nishida, Y.-M. Lee, W. Nam and S. Fukuzumi, *J. Am. Chem. Soc*., 2014, **136**, 8042.
48 F. Li, K. M. Van Heuvelen, K. K. Meier, E. Münck, L. Que, Jr., *J. Am. Chem. Soc*., 2013, **135**, 10198.
49 A. F. Rogério R. A. F. Tomás, J. C. M. Bordado and J. F. P. Gomes, *Chem. Rev*., 2013, **113**, 7421.
50 T. Yu and M. C. Lin, *J. Am. Chem. Soc*., 1994, **116**, 9571.
51 I. V. Tokmakov, G. Kim, V. V. Kislov, A. M. Mebel and M. C. Lin, *J. Phys. Chem. A*, 2005, **109**, 6114.
52 Y.-M. Lee, H. Kotani, T. Suenobu, W. Nam and S. Fukuzumi, *J. Am. Chem. Soc*., 2008, **130**, 434.
53 S. Fukuzumi, Y. Morimoto, H. Kotani, P. Naumov, Y.-M. Lee and W. Nam, *Nature Chem*., 2010, **2**, 756.
54 K. A. Prokop and D. P. Goldberg, *J. Am. Chem. Soc*., 2012, **134**, 8014.
55 J. Jung, K. Ohkubo, K. A. Prokop, H. M. Neu, D. P. Goldberg and S. Fukuzumi, *Inorg. Chem*., 2013, **52**, 13594-13604.
56 P. J. Gonçalves, L. De Boni, I. E. Borissevitch and S. C. Zílio, *J. Phys. Chem. A*, 2008, **112**, 6522.
57 E. Krokos, F. Spänig, M. Ruppert, A. Hirsch and D. M. Guldi, *Chem.–Eur. J*., 2012, **18**, 1328.
58 J. Jung, K. Ohkubo, D. P. Goldberg and S. Fukuzumi, *J. Phys. Chem. A*, 2014, **118**, 6223.
59 S. Fukuzumi, T. Mizuno and T. Ojiri, *Chem.–Eur. J*., 2012, **18**, 15794.
60 Gupta, R.; Borovik, A. S. J. Am. Chem. Soc. 2003, 125, 13234.
61 D. C. Lacy, R. Gupta, K. L. Stone, J. Greaves, J. W. Ziller, M. P. Hendrich and A. S. Borovik, *J. Am. Chem. Soc*., 2010, **132**, 12188.
62 J.-W. Rohde, J.-H. In, W. W. Brennessel, M. R. Bukowski, A. Stubna, E. Münck, W. Nam and L. Que, Jr., *Science*, 2003, **299**, 1037-1039.
63 J. England, Y. Guo, E. R. Farquhar, V. G. Young, Jr., E. Münck, L. Que, Jr., *J. Am. Chem. Soc*., 2010, **132**, 8635.

64 E. J. Klinker, J. Kaizer, W. W. Brennessel, N. L. Woodrum, C. J. Cramer, L. Que, Jr., *Angew. Chem., Int. Ed*., 2005, **44**, 3690.
65 Y. Nishida, Y. Morimoto, W. Nam, and S. Fukuzumi, *Inorg. Chem*., 2013, **52**, 3094.
66 Y. Hirai, T. Kojima, Y. Mizutani, Y. Shiota, K. Yoshizawa and S. Fukuzumi, *Angew. Chem., Int. Ed*., 2008, **47**, 5772.
67 T. Kojima, K. Nakayama, K. Ikemura, T. Ogura and S. Fukuzumi, *J. Am. Chem. Soc*., 2011, **133**, 11692.
68 S. Ohzu, T. Ishizuka, Y. Hirai, Y. Shiota, K. Yoshizawa, M. Sakaguchi, T. Ogura, H. Jiang, S. Takahashi, S. Fukuzumi and T. Kojima, *Chem. Sci*., 2012, **3**, 3421.
69 P. Barman, A. K. Vardhaman, B. Martin, S. J. Wörner, C. V. Sastri and Peter Comba, *Angew. Chem., Int. Ed*., **2015**, *53* in press DOI: 10.1002/anie.201409476.
70 J. J. Concepcion, J. W. Jurss, M. K. Brennaman, P. G. Hoertz, A. O. T. Patrocinio, N. Y. Murakami Iha, J. L. Templeton and T. J. Meyer, *Acc. Chem. Res*., 2009, **42**, 1954.
71 X. Sala, S. Maji, R. Bofill, J. Gárcia-Antón, L. Escriche and A. Llobet, *Acc. Chem. Res*., 2014, **47**, 504.
72 S. Fukuzumi, D. Hong and Y. Yamada, *J. Phys. Chem. Lett*., 2013, **4**, 3458.
73 A. R. Parent and K. Sakai, *ChemSusChem*, 2014, **7**, 2070.
74 L. Duan, L. Tong, Y. Xu and L. Sun, *Energy Environ. Sci*., 2011, **4**, 3296.
75 H. Lv, Y. V. Geletii, C. Zhao, J. W. Vickers, G. Zhu, Z. Luo, J. Song, T. Lian, D. G. Musaev and C. L. Hill, *Chem. Soc. Rev*., 2012, **41**, 7572.
76 J. M. Sumliner, H. Lv, John Fielden,Y. V. Geletii and C. L. Hill, *Eur. J. Inorg. Chem*., 2014, 635.
77 K. J. Young, L. A. Martini, R. L. Milot, R. C. Snoeberger III, V. S. Batista, C. A. Schmuttenmaer, R. H. Crabtree and G. W. Brudvig, *Coord. Chem. Rev*., 2012, **256**, 2503.
78 R. Cao, W. Lai and P. Du, *Energy Environ. Sci*., 2012, **5**, 8134.
79 D. G. H. Hetterscheid and J. N. H. Reek, *Angew. Chem., Int. Ed*., 2012, **51**, 9740.
80 D. J. Wasylenko, R. D. Palmer and C. P. Berlinguette, *Chem. Commun*., 2013, **49**, 218.
81 V. Artero and M. Fontecave, *Chem. Soc. Rev*., 2013, **42**, 2338.
82 S. Fukuzumi and D. Hong, *Eur. J. Inorg. Chem*., 2014, 645.
83 J. J. Stracke and R. G. Finke, *J. Am. Chem. Soc*., 2011, **133**, 14872.
84 Jordan J. Stracke and Richard G. Finke, *ACS Catal*., 2014, **4**, 909.
85 J. L. Fillol, Z. Codolà, I. Garcia-Bosch, L. Gómez, J. J. Pla and M. Costas, *Nat. Chem*., 2011, **3**, 807.
86 D. Hong, S. Mandal, Y. Yamada, Y.-M. Lee, W. Nam, A. Llobet and S. Fukuzumi, *Inorg. Chem*., 2013, **52**, 9522.
87 D. Hong, M. Murakami, Y. Yamada and S. Fukuzumi, *Energy Environ. Sci*., 2012, **5**, 5708.
88 D. Hong, J. Jung, J. Park, Y. Yamada, T. Suenobu, Y.-M. Lee, W. Nam and S. Fukuzumi, *Energy Environ. Sci*., 2012, **5**, 7606.
89 A. Sartorel, M. Carraro, G. Scorrano, R. De Zorzi, S. Geremia, N. D. McDaniel, S. Bernhard and M. Bonchio, *J. Am. Chem. Soc*., 2008, **130**, 5006.
90 Y. V. Geletii, B. Botar, P. Kögerler, D. A. Hillesheim, D. G. Musaev and C. L. Hill, *Angew. Chem., Int. Ed*., 2008, **47**, 3896.
91 Q. Yin, J. M. Tan, C. Besson, Y. V. Geletii, D. G. Musaev, A. E. Kuznetsov, Z. Luo, K. I. Hardcastle and C. L. Hill, *Science*, 2010, **328**, 342.
92 J. W. Vickers, H. Lv, J. M. Sumliner, G. Zhu, Z. Luo, D. G. Musaev, Y. V. Geletii and C. L. Hill, *J. Am. Chem. Soc*., 2013, **135**, 14110.
93 X.-B. Han, Z.-M. Zhang, T. Zhang, Y.-G. Li, W. Lin, W. You, Z.-M. Su and E.-B. Wang, *J. Am. Chem. Soc*., 2014, **136**, 5359.
94 Y. Cui, L. Shi, Y. Yang, W. You, L. Zhang, Z. Zhu, M. Liu and L. Sun, *Dalton Trans*., 2014, **43**, 17406.
95 M. Murakami, D. Hong, T. Suenobu, S. Yamaguchi, T. Ogura and S. Fukuzumi, *J. Am. Chem. Soc*., 2011, **133**, 11605.
96 S. Fukuzumi, T. Kishi, H. Kotani, Y.-M. Lee and W. Nam, *Nature Chem*., 2011, **3**, 38.
97 J. Berglund, T. Pascher, J. R. Winkler and H. B. Gray, *J. Am. Chem. Soc*., 1997, **119**, 2464.
98 C. E. Immoos, A. J. Di Bilio, M. S. Cohen, W. Van der Veer, H. B. Gray and P. J. Farmer, *Inorg. Chem*., 2004, **43**, 3593.
99 H. Kotani, T. Suenobu, Y.-M. Lee, W. Nam and S. Fukuzumi, *J. Am. Chem. Soc*., 2011, **133**, 3249.
100 J. Park, Y. Morimoto, Y.-M. Lee, W. Nam and S. Fukuzumi, *J. Am. Chem. Soc*., 2011, **133**, 5236.
101 J. Park, Y. Morimoto, Y.-M. Lee, W. Nam and S. Fukuzumi, *J. Am. Chem. Soc*., 2012, **134**, 3903.
102 S. Ohzu, T. Ishizuka, Y. Hirai, S. Fukuzumi and T. Kojima, *Chem.–Eur. J*., 2013, **19**, 1563.
103 D. Chao and W.-F. Fu, *Dalton Trans*., 2014, **43**, 306.

Graphics for TOC

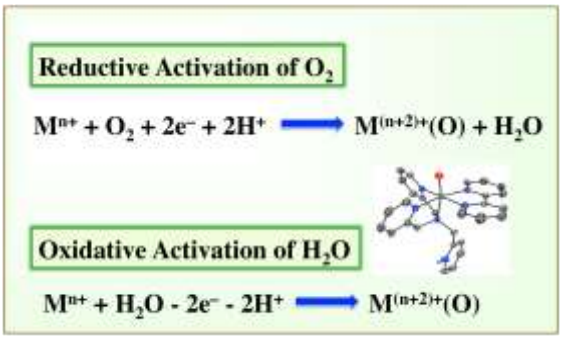

High-valent metal-oxo complexes are produced by thermal and photoinduced electron-transfer reactions, acting as catalysts for for oxygenation of substrates using water or dioxygen as an oxygen source.